Hydrological Effects on the Air-Ocean Coupled System

Pecheng C. CHU and Roland W. GARWOOD, Jr

Department of Oceanography, Naval Postgraduate School
Monterey, CA 93943 - U.S.A.

ABSTRACT

The ocean and atmosphere are driven by the fluxes of momentum, heat, and water mass. The importance of the fluxes of momentum and heat is well recognized by both meteorologists and oceanographers. The hydrological cycle is, however, only given considerable attention in atmospheric models since the latent heat release is an important source of the atmospheric general circulation. The hydrological cycle is given less attention in ocean models although it is realized that evaporation and precipitation are contributors to the surface buoyancy flux which determines the depth of mixing and drives the thermohaline circulation.

The cloud and the ocean mixed layer are highly coupled by both the heat and moisture fluxes across the air-ocean interface. Two time scales are found in this paper: a sea surface temperature (SST) time scale, τ_T, that is virtually controlled by the oceanic planetary boundary layer (OPBL), and a cloud-SST coupling time scale, $\tau_{n,T}$. These two time scales depend on the stability of the marine atmospheric boundary layer (MABL).

An air-ocean model is developed in this paper for the coupled system of an unstable atmosphere overlying a stable ocean. The model results demonstrate that the exchanges of heat and water fluxes across the sea surface leads to both growing and decaying modes of oscillation on 3-6 day and 20-30 day time scales. These oscillatory solutions are entirely thermodynamic and do not require wave dynamics for their existence.

1. Introduction

Since 1970 significant progress has been made both in our ability to carry out air-sea interaction field work and in our understanding of many of the processes found on both sides of the air-sea interface. Many studies, both observational and theoretical, have shown that the surface wind and the SST are two important elements in the air-sea coupled system (Chu, 1989). Since clouds have significant effects on the large-scale atmospheric circulation through the transfer of heat and moisture, and on the OPBL through the attenuation of the solar radiation at the ocean surface, there may be strong feedback between the clouds and the OPBL. Fig.1 shows the main physical processes (heat, mass, and momentum fluxes) at the two adjacent boundary layers: the OPBL and the marine atmospheric boundary layer (MABL). Fig.2 illustrates the feedback pathways between the clouds and the ocean mixed layer.

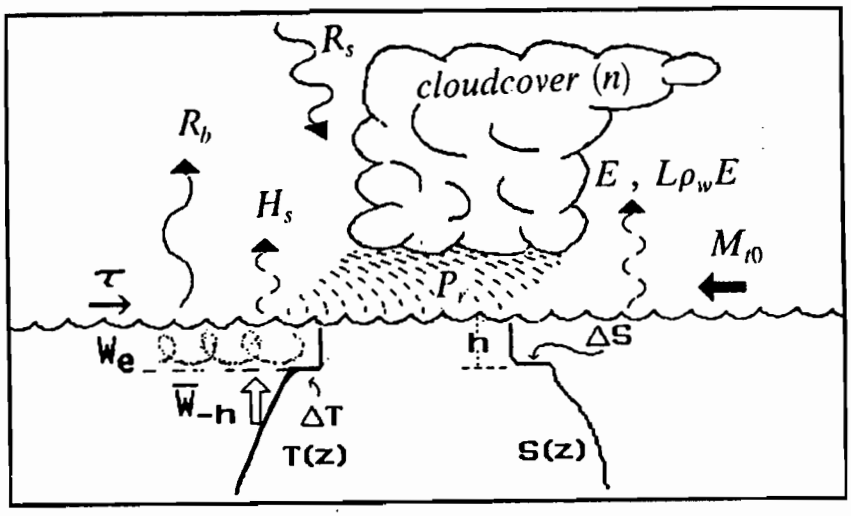

Fig.1 Main physical processes at the two adjacent boundary layers.

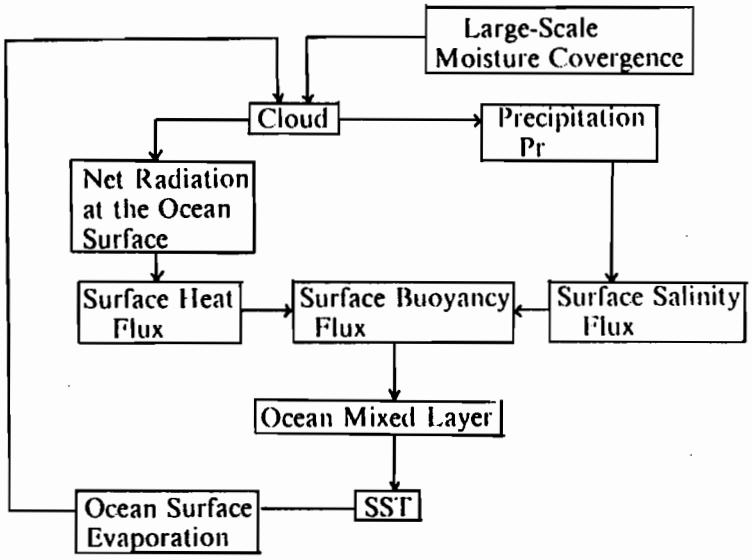

Fig.2 Feedback paths between OPBL and clouds.

The feedback mechanism between clouds and ocean mixed layer in the buoyant forcing regime (upward buoyancy flux at the ocean surface) was illustrated by Chu and Garwood (1989). However, the TOGA (Tropical Ocean Global Atmosphere Program) observations have shown the warm pool regions of the western Pacific to be in the buoyant damping regime (downward buoyancy flux) for the OPBL due to fresh water influx caused by an excess of precipitation over evaporation. The OPBL is usually stable, and the MABL is generally unstable. Therefore, the feedback mechanism in this coupled system (unstable MABL - stable OPBL) should have different form from the buoyant forcing case.

Although our coupled model is one-dimensional, we are aware of the importance of the horizontal advection and the limitation of one-dimensional models. However, the intent of this work is to develop a formalism to examine thermodynamic feedback between the two fluids. Because we wish to concentrate on the thermodynamic interaction, horizontal advection is ignored initially.

2. Similarity Functions in the MABL

According to the similarity theory it is assumed that if a variable (wind, temperature, or moisture, etc.) is appropriately scaled, then its profile follows a universal function whose form, in general, is determined empirically. For the barotropic atmosphere the appropriate scales for wind and height are

$$U = U_g, \quad h_a = \frac{\alpha u_{a^*}}{|f|} \tag{1}$$

where U_g is the geostrophic wind speed, which is assumed here to be $10 m/s$, u_{a^*} is the atmospheric friction velocity. The geostrophic drag coefficient C_g is defined by Yamada (1976) as

$$C_g = \frac{u_{a^*}}{|U_g|} = \kappa\{[\ln(\frac{h_a}{z_0}) - A]^2 + B^2\}^{-1/2} \tag{2}$$

where κ is the von Karman constant, 0.4. The roughness parameter, z_0, is approximately $1.5 \times 10^{-4} m$. The ratio h_a/z_0 is 0.6×10^7 for an MABL height, $h_a = 1 km$. The heat and moisture transfer coefficients are determined by

$$C_H = -\frac{\overline{w'_a \theta'}|_0}{u_{a^*}[\hat{\theta} - \theta(z_0)]}, \quad C_E = -\frac{\overline{w'_a q'}|_0}{u_{a^*}[\hat{q} - q(z_0)]} \tag{3}$$

where w, θ, q are the vertical velocity, potential temperature, and specific humidity, respectively. The superscript " ' " means the disturbance, and " $\wedge$ " indicates the values being taken at the top of the MABL. The heat transfer coefficient is further computed by Yamada (1976) as

$$C_H = = \frac{\kappa}{Pr_0}[\ln(\frac{h}{z_0}) - C]^{-1} \tag{4}$$

where Pr_0 is the turbulent Prandtl number for neutral stability, having a value of 0.74 according to Businger et al. (1971). Based on the Wangara data, the similarity functions A, B, C are experimentally determined by Yamada (1976) for the stable atmosphere:

$$A = 1.855 - 0.38 h_a/L_a \quad (0 \le h_a/L_a \le 35),$$

$$A = -2.94(h_a/L_a - 19.94)^{1/2} \quad (35 < h_a/L_a);$$

$$B = 3.02 + 0.3 h_a/L_a \quad (0 \le h_a/L_a \le 35),$$

$$B = 2.85(h_a/L_a - 12.47)^{1/2} \quad (35 < h_a/L_a);$$

$$C = 3.665 - 0.829 h_a/L_a \quad (0 \le h_a/L_a \le 18),$$

$$C = -4.23(h_a/L_a - 11.21)^{1/2} \quad (18 < h_a/L_a) \tag{5a}$$

and for the unstable atmosphere ($h_a/L_a < 0$)

$$A = 10.0 - 8.145(1 - 0.008376 h_a/L_a)^{-1/3},$$

$$B = 3.02(1 - 3.29 h_a/L_a)^{-1/3},$$

$$C = 12.0 - 8.335(1 - 0.03106h_a/L_a)^{-1/3} \tag{5b}$$

where L_a is the atmospheric Obukhov length scale. The computation for the moisture transfer coefficient is not very clear yet. In this paper we assume that

$$C_E = C_H \tag{6}$$

Substitution of (5 a,b) into (2) and (4) leads to the apparently strong dependence of C_g, C_H, C_E on the atmospheric stability parameter h_a/L_a, as shown in Fig.3. These parameters have much larger values for the unstable than for the stable atmosphere, i.e.,

$$C_g \sim 0.0316, \quad C_H, C_E \sim 0.063 \quad (h_a/L_a < 0)$$

$$C_g \sim 0.003, \quad C_H, C_E \sim 0.004 \quad (h_a/L_a > 0) \tag{7}$$

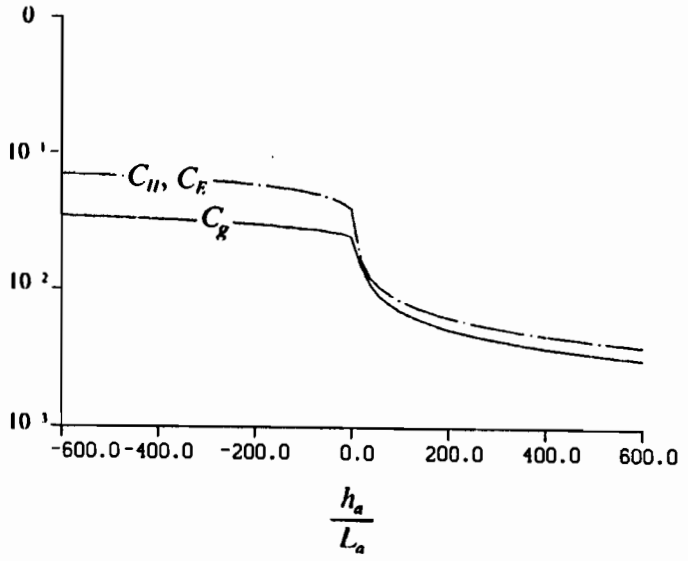

Fig.3 Dependence of C_g, C_H, C_E on the atmospheric stability parameter (h_a/L_a).

3. Time Rate of Change of the Cloud Cover

The time rate of change of cloud cover is assumed to be proportional to the moisture supply divided by the amount of water vapor necessary to produce the model cloud. The main processes causing the cloud dissolution are precipitation and mixing with the environmental air. The cloud evaporation due to mixing with ambient air is a complicated problem, and is neglected for the sake of simplicity here. Thus the equation for cloud cover is

$$\frac{\partial n}{\partial t} = \frac{(M_{t0} + E - P_r)}{h_c} \tag{8}$$

where h_c is the total amount of water vapor needed to create the cloud over a unit area. From mean distributions of temperature and mixing ratio in the environmental air outside the cloud and inside a deep cumulus cloud (Kuo, 1965), we estimate that $h_c \sim 5$ *cm*. The large-scale horizontal moisture convergence in the column of atmosphere per unit area is denoted M_{t0}.

4. Relationship between Precipitation Rate and Cloud Cover

By linear regression of hourly rain amounts and satellite IR brightness data obtained during Phases I, II, and III of GATE, Albright et al. (1985) presented a linear relationship between average precipitation rate P_r in boxes 1.5° (168 km) on a side and cloud cover n of the boxes by clouds with tops colder than −36° C:

$$P_r(ms^{-1}) = (0.472 + 8.333\, n) \times 10^{-7} \tag{9}$$

This result confirms Arkin's (1979) earlier analysis for the GATE B-scale array.

5. Ocean Mixed Layer

Much of the one-dimensional theory for the OPBL or mixed layer is dependent upon the validity of two crucial hypotheses. The first of these is that vertical mixing within the turbulent boundary layer and entraiment mixing at its base occur in response to the local atmospheric forcing - the surface wind stress and the buoyancy flux at the sea surface. The second hypothesis is that the mechanical energy budget is the key to the understanding and prediction of mixed layer dynamics (Garwood, 1977, 1979).

The buoyancy flux is attributable to heat flux, evaporation, and precipitation. The shear production of turbulence is attributable to surface wind stress. In the western Pacific warm pool regions, the excess precipitation effect prevails over the buoyancy effect of heat lost at the ocean surface, causing the net buoyant flux to be downward. The mixed layer depth equals the Obukhov length scale:

$$h_w = L_w = \frac{2u_{w*}^3}{B} \tag{10}$$

where L_w is the oceanic Obukhov length scale. The oceanic friction velocity is

$$u_{w*} = \left(\frac{\rho_a}{\rho_w}\right)^{1/2} u_{a*}$$

and B is the downward surface buoyancy flux

$$B \equiv \beta g S(P_r - E) - \frac{\alpha g F}{\rho_w c_{pw}} \tag{11}$$

where ρ_a, ρ_w are the air and sea water densities, α is the sea water thermal expansion coefficient, and β is the salinity contraction coefficient. Because the OPBL is in the buoyant damping regime, the mixed layer heat and salinity budgets include no entrainment:

$$\frac{\partial T_w}{\partial t} = -\frac{F}{\rho_w c_p^{(w)} h_w} - A_T \tag{12}$$

$$\frac{\partial S}{\partial t} = +\frac{(E - P_r)S}{h_w} - A_S \tag{13}$$

where $c_p^{(w)}$ is the specific heat under constant pressure. The parameters A_T and A_S are the horizontal advection for temperature and salinity, respectively.

The effects of clouds on the buoyancy flux at the ocean surface are two-fold: (1) decreasing B_0 through the increase in the net heat loss at the ocean surface, F, by reducing the incoming solar radiation, and (2) increasing B_0 due to precipitation. The net heat loss from the ocean surface is given by

$$F = R_b - R_s + \rho_a c_{pa} C_g U_G C_H [T_w - \hat{\theta}] + L\rho_a C_g U_G C_E [q_s(T_w) - \hat{q}] \qquad (14)$$

where q_s(T) is the saturated mixing ratio. The incoming solar radiation absorbed by the ocean surface is R_s, and R_b is the net energy loss from the ocean surface by longwave radiation, L is the latent heat of vaporization of water, and H_s is the sensible heat flux to the air. The standard bulk formulae are used to calculate the surface evaporation:

$$E = \rho_a C_g U_g C_E [q_s(T_w) - \hat{q}]/\rho_w \qquad (15)$$

6. Cloud Effects on the Net Radiation at the Ocean Surface

Clouds reduce the solar radiation incident at the ocean surface by scattering and absorption, which is computed by Budyko's (1978) formula

$$R_s = [1 - \alpha_{sn} n - \alpha_{s0}(1 - n)]R_{s0} \qquad (16)$$

Here R_{s0} (340 W m^{-2}) is the solar radiation absorbed by the ocean surface layer under a clear sky. The parameters α_{sn} and α_{s0} represent albedos of the earth-atmosphere system with complete cloud cover and a cloudless sky, respectively, and have the following values:

$$\alpha_{sn} = 0.46, \qquad \alpha_{s0} = 0.2$$

The ocean surface emits longwave radiation to the atmosphere and to space. However, clouds, as well as dry air, partially absorb the radiation and re-emit longwave radiation back to the ocean surface. Thus the net upward energy loss by longwave radiation at the ocean surface, R_b, is corrected for the downward radiation by the clouds and the air. From longwave radiation data, Budyko (1978) derived a semi-emprical formula:

$$R_b = a + bT - (a_1 + b_1)n \qquad (17)$$

The dimensional coefficients a, b, a_1, and b_1 are

$$a = -377.6\ Wm^{-2},\ b = 2.2\ Wm^{-2}K^{-1},$$

$$a_1 = -389.8\ Wm^{-2}, b_1 = 1.6\ Wm^{-2}K^{-1}$$

7. Basic Equations for Perturbations

When the coupled system is perturbed from its equilibrium state, the thermodynamic feedback mechanism between the cumulus clouds and the oceanic mixed layer makes the perturbation either grow (positive feedback) or dampen (negative feedback). The principal purpose here is to study thermodynamic feedback mechanisms between clouds and the oceanic mixed layer. Hence the energy exchange at the air-ocean interface is a primary focal point. Therefore, we shall neglect initially the perturbations of those variables which are not di-

rectly related to the exchange at the air-ocean interface. From the basic equations of the coupled system (8), (10), (12), and (13), the perturbations satisfy the following equations:

$$\frac{\partial n'}{\partial t} = \frac{1}{\bar{h}_c}\left(\frac{\partial E}{\partial T_w} T'_w - \frac{\partial \bar{P}_r}{\partial n} n'\right) \tag{18}$$

$$h'_w = -\frac{\bar{h}_w}{\bar{B}} B' = \frac{\bar{h}_w}{\bar{B}}\left[\left(\frac{\alpha g}{\rho_w c_{pw}} \frac{\partial \bar{F}}{\partial T_w} + \beta g \bar{S} \frac{\partial \bar{E}}{\partial T_w}\right) T'_w\right.$$

$$\left. - \beta g \bar{S}(\bar{P}_r - \bar{E}) S' + \left(\frac{\alpha g}{\rho_w c_{pw}} \frac{\partial \bar{F}}{\partial n} - \beta g \bar{S} \frac{\partial \bar{P}_r}{\partial n}\right) n'\right] \tag{19}$$

$$\frac{\partial T'_w}{\partial t} = -\frac{1}{\rho_w c_p^{(w)} \bar{h}_w}\left(\frac{\partial \bar{F}}{\partial n} n' + \frac{\partial \bar{F}}{\partial T_w} T'_w + \frac{\bar{F} h'_w}{\bar{h}_w}\right) \tag{20}$$

$$\frac{\partial S'}{\partial t} = \frac{(\bar{E} - \bar{P}_r)}{\bar{h}_w} S' + \frac{\bar{S}}{\bar{h}_w}(E' - P'_r) + \frac{(\bar{P}_r - \bar{E})\bar{S}}{\bar{h}_w^2} h'_w \tag{21}$$

8. Three Basic Time Scales

Three time scales are found from (18)-(21):

Cloud time scale

$$\tau_n^{-1} = \frac{1}{h_c} \frac{\partial \bar{P}_r}{\partial n} \tag{22}$$

Using (9) and taking $h_c = 5cm$, we have

$$\tau_n \sim 0.6 \ day \tag{23}$$

SST variation time scale

$$\tau_T^{-1} \equiv \frac{1}{\rho_w c_{pw} \bar{h}_w} \frac{\partial \bar{F}}{\partial T_w} \tag{24}$$

The net heat loss from the ocean surface is computed by (14). Assuming that $\hat{\theta}$ and $\hat{q}$ are determined by the large-scale atmospheric motion, we have

$$\frac{\partial \bar{F}}{\partial T_w} = \rho_a c_{pa} U_g \left(1 + \frac{L^2 q_s}{c_{pa} R_v T_w^2} \frac{C_E}{C_H}\right) C_g C_H$$

therefore

$$\tau_T^{-1} = \frac{\rho_a c_{pa} U_g}{\rho_w c_{pw} \bar{h}_w}\left(1 + \frac{L^2 q_s}{c_{pa} R_v T_w^2} \frac{C_E}{C_H}\right) C_g C_H \tag{25}$$

Cloud and SST coupling time scale

$$\tau_{n,T}^{-1} \equiv \frac{1}{\rho_w c_{pw} \bar{h}_w} \frac{\partial \bar{F}}{\partial n} \frac{\partial \bar{E}}{\partial T_w} / \frac{\partial \bar{P}_r}{\partial n} \tag{26}$$

Substitution of (22) into (26) leads to

$$\tau_{n,T}^{-1} = [\frac{\tau_n U_G L q_s \frac{\partial F}{\partial n}}{\rho_w c_{pw} h_w h_c R_v T_w^2}] C_g C_E \tag{27}$$

Using (16) and (17) we have

$$\frac{\partial F}{\partial n} = \frac{\partial (R_b - R_s)}{\partial n} \sim 15 Wm^{-2}$$

Among these three time scales, τ_n is the shortest. The other two, τ_T and $\tau_{n,T}$, largely depend on the parameters C_g, C_H, and C_E, which are functions of the atmospheric stability. Fig.4 shows the dependence of τ_T and $\tau_{n,T}$ on the atmospheric stability. For the unstable atmosphere ($h_a/L_a < 0$), $\tau_{n,T} \sim 3 - 6$ days, and $\tau_T \sim 20 - 30$ days. For the stable atmosphere ($h_a/L_a > 0$), $\tau_{n,T} \sim 0.3 - 1$ years, and $\tau_T \sim 1 - 3$ years.

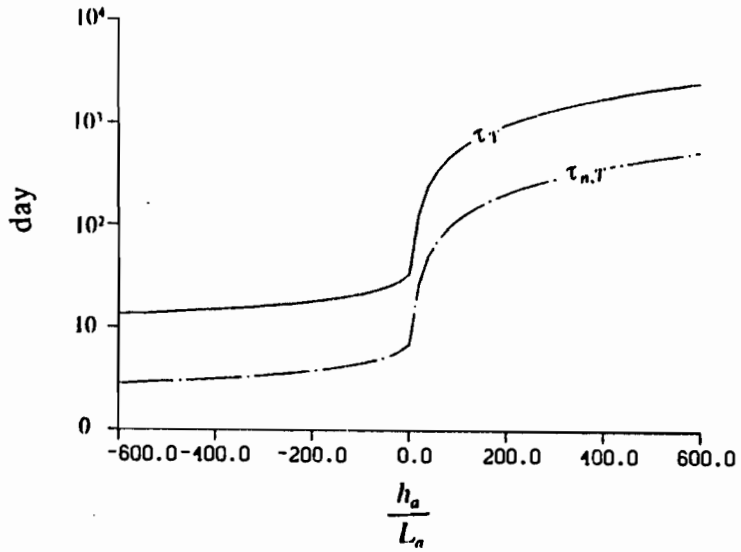

Fig.4 Dependence of τ_T and $\tau_{n,T}$ on the atmospheric stability parameter h_a/L_a).

9. Solutions

Since the time scale for cloud feedback is so much shorter than that for SST feedback, i.e., $\tau_n \ll \tau_T$, the cloud cover perturbation, n', almost instantaneously follows the SST for the temperature feedback:

$$n' = \frac{\partial \bar{E}/\partial T_w}{\partial \bar{P}_r/\partial n} T'_w \tag{28}$$

Eq.(9) shows that

$$\frac{\partial \bar{P}_r}{\partial n} \sim 8.33 \times 10^{-7} m s^{-1},$$

and for $\overline{T}_w = 25°C$, $u_{a*} = 0.1 m/s$,

$$\frac{\partial \overline{E}}{\partial T_w} = C_E u_{a*} \frac{dq_s(z_0)}{dT_w} \sim 4.63 \times 10^{-7} ms^{-1} K^{-1}.$$

Therefore, a $1°C$ change in SST implies a 0.56 change in cloud cover.

Neglecting the small terms in the prognostic equations for T'_w and S' and eliminating three among the four variables n', T'_w, S', and h'_w from (19), (20), (21), (28), we obtain the second order differential equation,

$$\frac{\partial^2 \psi}{\partial t^2} - \frac{2\mu - \gamma}{\gamma - \mu}(\tau_{n,T}^{-1} + \tau_T^{-1}) \frac{\partial \psi}{\partial t} + \frac{\mu\gamma^2}{(\gamma - \mu)^2}(\tau_{n,T}^{-1} + \tau_T^{-1})^2 \psi = 0 \tag{29}$$

where ψ represents n', T'_w, S', and h'_w. There are two nondimensional parameters,

$$\mu = \frac{4\alpha g \overline{F}/\rho_w c_{pw}}{\beta g \overline{h}_w \overline{S}(\tau_{n,T}^{-1} + \tau_T^{-1})}, \quad \gamma = \frac{4\beta g(\overline{P}_r - \overline{E})\overline{S}}{\beta g \overline{h}_w \overline{S}(\tau_{n,T}^{-1} + \tau_T^{-1})} \tag{30}$$

that indicate the relative importance of mean heat and mean salinity fluxes in the mean surface buoyancy flux (11). The general solutions of (29) have the form:

$$\psi = C_1 \exp(\sigma_1 t) + C_2 \exp(\sigma_2 t) \tag{31}$$

where C_1 and C_2 are integral constants, and σ_1 and σ_2 are the eigenvalues which are the roots of the second-order algebraic equation

$$\sigma^2 - \frac{2\mu - \gamma}{\gamma - \mu}(\tau_{n,T}^{-1} + \tau_T^{-1})\sigma + \frac{\mu\gamma^2}{(\gamma - \mu)^2}(\tau_{n,T}^{-1} + \tau_T^{-1})^2 = 0 \tag{32}$$

10. Instability and Oscillation Criteria

The instability criteria for the thermodynamically coupled air-ocean system are

$$Re(\overline{\sigma}) \begin{cases} < 0 & \textit{decaying} \\ = 0 & \textit{neutral,} \\ > 0 & \textit{growing} \end{cases} \tag{33}$$

where $\overline{\sigma}$ is σ_1 or σ_2, the root of the second-order equation (32). The oscillatia criterion for the coupled system are

$$Im(\overline{\sigma}) \begin{cases} = 0 & \textit{nonoscillatory} \\ \neq 0 & \textit{oscillatory} \end{cases} \tag{34}$$

The roots σ_1 and σ_2 are

$$\sigma_{1,2} = \frac{(2\mu - \gamma)}{2(\overline{\gamma} - \mu)}(\tau_{n,T}^{-1} + \tau_T^{-1})[1 \pm \sqrt{(1 - \mu\gamma^2/(2\mu - \gamma)^2} \tag{35}$$

The condition for the generation of growing/decaying modes, which can be deduced from (38), is:

$$\frac{2\mu-\gamma}{\gamma-\mu} \quad \begin{cases} < 0 & \textit{decaying} \\ = 0 & \textit{neutral,} \\ > 0 & \textit{growing} \end{cases} \tag{36}$$

and the condition for oscillatory/nonoscillatory modes is:

$$(1-\frac{2\mu}{\gamma})^2 \quad \begin{cases} > \mu & \textit{nonoscillatory} \\ < \mu & \textit{oscillatory} \end{cases} \tag{37}$$

Separation of different modes in the $\gamma-\mu$ plane is shown in Fig.5. For the buoyant damping regime ($\overline{B}>0$, i.e., $\gamma>\mu>0$) which corresponds to the western Pacific warm pool regime, the relative importance of the mean surface heat and salinity fluxes in the mean buoyancy flux $\overline{B}$ is a key factor controling the modes of the coupled air-ocean system. The mean surface salinity flux, measured by γ, makes the upper ocean more buoyant (stabilizing factor), however, the mean upward heat flux, measured by μ, makes the upper ocean less buoyant (destabilizing factor). The larger the parameter γ (μ), the stronger the negative (positive) feedback mechanism. Combining (36) and (37) leads to the same results:

$$\gamma > \frac{2\mu}{1-\sqrt{\mu}} \qquad \Rightarrow \textit{Nonoscillatory Damping}$$

$$\frac{2\mu}{1-\sqrt{\mu}} > \gamma > 2\mu \qquad \Rightarrow \textit{Oscillatory Damping}$$

$$2\mu > \gamma > \frac{2\mu}{1+\sqrt{\mu}} \qquad \Rightarrow \textit{Oscillatory Growing}$$

$$\frac{2\mu}{1+\sqrt{\mu}} > \gamma > \mu \qquad \Rightarrow \textit{Nonoscillatory Growing} \tag{38}$$

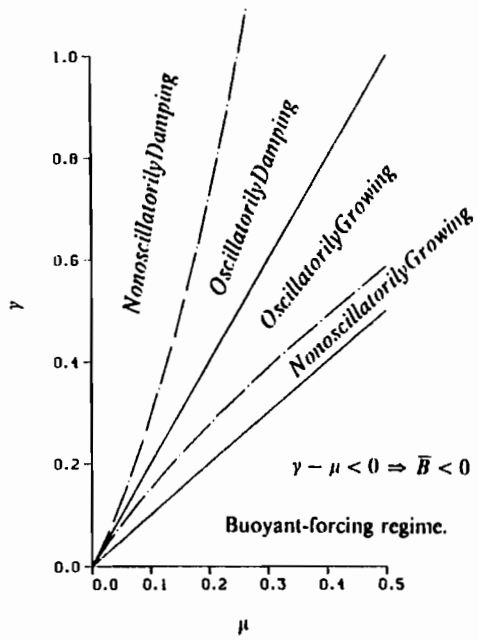

Fig.5 Separation of different modes in the (γ, μ) plane.

11. Conclusion

The feedback between the cloud and OPBL in the coupled MABL and stable OPBL system is investigated by a coupled model. The time scales largely depend on the stability of the MABL. For the stable atmosphere, the two time scales are quite long: $\tau_T \sim$ 100-300 days, and $\tau_{n,T} \sim$ 1-3 yr. For the unstable atmosphere, however, the two time scales are much shorter: $\tau_T \sim$ 3-6 days, and $\tau_{n,T} \sim$ 20-30 days. In the western Pacific warm pool regions, the MABL is usually unstable. Therefore, this theory may provide some explanation of the two time scales (3-6 and 20-30 days) of intense convection in the western Pacific.

In the coupled system, the fresh water influx at the ocean surface due to the excess precipitation over evaporation is a damping factor (negative feedback). However, the surface cooling is a forcing factor (positive feedback). The relative strengths of these two surface fluxes determine the mode type: decaying or growing, oscillatory or nonoscillatory.

Acknowledgements.

This research was supported by the National Science Foundation, the Office of Naval Research, and the U.S. Naval Postgraduate School.

REFERENCES

Albright, M.D., E.E. Recker, R.J. Reed, and R.Q. Dang, 1985: The diurnal variation of deep convection and inferred precipitation in the central tropical Pacific during January-February 1979. Mon. Wea. Rev., **113,** 1663-1680.

Arkin, P.A., 1979: The relationship between fractional coverage of high cloud and rainfall accumulations during GATE over the B-scale array. Mon. Wea. Rev., **107,** 1382-1387.

Budyko, M.I., 1978: The heat balance of the earth. Climatic Change (ed. J. Gribbin), Cambgidge Univ. Press, 85-113.

Chu, P.C., 1989: Relationship between thermally forced surface wind and sea surface temperature gradient. Pure & Appl. Geophys., **130,** 31-45.

Chu, P.C., and R.W. Garwood, Jr., 1988: Comment on "A coupled dynamic-thermodynamic model of an ice-ocean in the marginal ice zone" by Sirpa Hakkinen. J. Geophys. Res., **93,** 5155-5156.

Chu, P.C., and R.W. Garwood, Jr., 1989: Cloud - ocean mixed layer feedback. AMS Symposium on the Role of Clouds in Atmospheric Chemistry and Global Climate, 39-44.

Garwood, R.W. Jr., 1977: An oceanic mixed layer capable of simulating cyclic states. J. Phys. Oceanogr., **7,** 455-468.

Garwood, R.W. Jr., 1979: Air-sea interaction and dynamics of the surface mixed layer. Rev. Geophys. Space Phys., **17,** 1507-1524.

Kuo, H.L., 1965: On formation and intensification of tropical cyclones through latent heat release by cumulus convection. J. Atmos. Sci., **22,** 40-63.

Yamada, T., 1976: On the similarity functions A, B, and C of the planetary boundary layer. J. Atmos. Sci., **33,** 781-793.

WESTERN PACIFIC INTERNATIONAL MEETING AND WORKSHOP ON TOGA COARE

Nouméa, New Caledonia
May 24-30, 1989

PROCEEDINGS

edited by

Joël Picaut *
Roger Lukas **
Thierry Delcroix *

* ORSTOM, Nouméa, New Caledonia
** JIMAR, University of Hawaii, U.S.A.

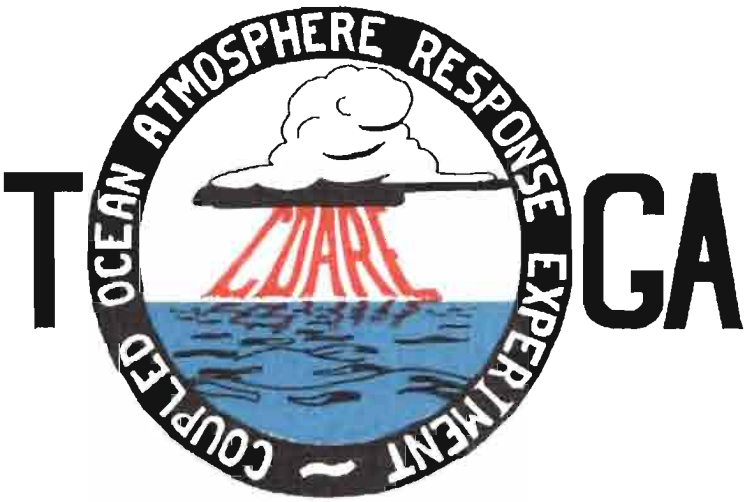

INSTITUT FRANÇAIS DE RECHERCHE SCIENTIFIQUE
POUR LE DÉVELOPPEMENT EN COOPÉRATION

ORSTOM

Centre de Nouméa

TABLE OF CONTENTS

MEETING COLLECTED PAPERS

WATER MASSES, SEA SURFACE TOPOGRAPHY, AND CIRCULATION

EL NINO/SOUTHERN OSCILLATION 1986-87

THEORETICAL AND MODELING STUDIES OF ENSO AND RELATED PROCESSES

MOMENTUM, HEAT, AND MOISTURE FLUXES BETWEEN ATMOSPHERE AND OCEAN

EMPIRICAL STUDIES OF ENSO AND SHORT-TERM CLIMATE VARIABILITY